



Daily dissolved oxygen saturation patterns mediated by light and stream discharge in littoral regions of an oligotrophic mountain lake

Heili E. Lowman^{1,2} · Kelly Loria^{1,3} · Leon Katona¹ · Jasmine Krause^{1,4} · Sudeep Chandra⁵ · Sally MacIntyre⁶ · John M. Melack⁶ · Ramon Naranjo⁷ · Joanna R. Blaszczak¹

Received: 17 December 2025 / Accepted: 9 March 2026
© The Author(s), under exclusive licence to Springer Nature Switzerland AG 2026

Abstract

Nearshore regions of lakes span ecosystem boundaries—terrestrial–aquatic, lotic–lentic, littoral–pelagic—and integrate signals that propagate across these boundaries, yet these regions are undersampled relative to pelagic waters. To examine controls on littoral ecosystem function, we measured high-frequency dissolved oxygen data along the shore of a large, oligotrophic lake during 2 years. We identified two distinct diel oxygen patterns—one whose peak was synchronous with solar noon and another whose peak lagged solar noon—that were distinguished as well by their overall magnitude of dissolved oxygen. We found that these diel oxygen patterns were correlated most strongly with daily light availability when sensors were deployed along a depth gradient and with stream discharge when sensors were in locations close to or far from inflowing streams. These results show that nearshore dissolved oxygen responds variably to climate and physical conditions, that is, light and discharge, depending on the location along the shore. Our approach further highlights the need to apply diverse quantitative methods to develop a better understanding of variability in littoral lake productivity in response to changing environmental conditions, particularly in oligotrophic lakes with low productivity signals that are typically challenging to detect.

Keywords Littoral · Lake · Oxygen · Nearshore · Light · Discharge

Introduction

Nearshore regions in lakes are increasingly recognized as distinct ecosystems and examining their function is of particular interest owing to their inclusion of multiple ecosystem boundaries. Littoral regions (i.e., where 1% of surface light reaches maximum water depth) are connected to pelagic regions by way of physical mixing and entrainment of deeper water onshore owing to wind and rates of cooling (MacIntyre et al. 2002), with the extent of mixing and exchange across the littoral–pelagic interface mediated by the degree of stratification (MacIntyre and Melack 1995). Benthic processes may exert an outsized influence on nearshore littoral ecosystem function owing to light availability and heterogeneous substrates fueling high metabolic rates (Sadro et al. 2011; Vadeboncoeur and Lowe 2024), increased resuspension of materials (MacIntyre and Melack 1995), and higher connectivity to groundwater inflows that deliver dissolved nutrients across the sediment–water interface (Naranjo et al. 2019; Vadeboncoeur et al. 2021). In addition to within-lake attributes, inflowing streams transmit water, organic matter,

✉ Heili E. Lowman
heili.lowman@duke.edu

¹ Department of Natural Resources and Environmental Science, University of Nevada Reno, Reno, NV 89557, USA

² Department of Biology, Duke University, Durham, NC 27708, USA

³ Desert Research Institute, University of Nevada Reno, Reno, NV 89557, USA

⁴ Department of Biological and Ecological Engineering, Oregon State University, Corvallis, OR 97331, USA

⁵ Department of Biology, University of Nevada Reno, Reno, NV 89557, USA

⁶ Department of Ecology, Evolution, and Marine Biology, University of California Santa Barbara, Santa Barbara, CA 93106, USA

⁷ Nevada Water Science Center, US Geological Survey, Carson City, NV 89701, USA

and dissolved materials from the surrounding watershed and airshed into lakes (Ward et al. 2022). Changes in hydroclimate (e.g., snowmelt timing) may lead to altered phenology of snowmelt (Kirchner et al. 2020; Siirila-Woodburn et al. 2021) and altered delivery of stream discharge to nearshore littoral regions (Cortés et al. 2014a, 2014b). Littoral dissolved oxygen (DO) patterns are known to respond to the combined effects of these abiotic and biotic processes, but it is unclear how signals vary seasonally and spatially (i.e., with depth and proximity to inflowing streams).

Globally, lakes are influenced by a changing climate, altering incoming fluxes of water and materials (Woolway et al. 2020; Vadeboncoeur et al. 2021) and affecting lake ecosystem function and water quality (Loewen 2023). In particular, oligotrophic lakes in mountain landscapes are vulnerable to climate change given their dependence on incoming snowmelt (Williamson et al. 2009; Moser et al. 2019). Mountain lakes are also sensitive to discrete weather events, such as rainstorms or high flow events, which can rapidly alter turbidity and light availability (Sadro and Melack 2012); antecedent conditions, such as drought and warming, have been shown to influence the impacts of such events on lake ecosystem function, with uncertain consequences for lakes experiencing changes in both the frequency and intensity of hydroclimatic disturbances (Perga et al. 2018; Oleksy et al. 2022). One method frequently used to quantify lake ecosystem function is to estimate primary productivity (i.e., metabolism) from changes in dissolved oxygen (DO; Jankowski et al. 2021), but these estimates are challenging to generate and uncertain in oligotrophic lakes where productivity is generally low (Staehr et al. 2010). When estimating productivity proves challenging, examining changes in the temporal signature of DO in oligotrophic lakes may provide useful ecological insights, as diel patterns in DO reflect the biology (i.e., metabolism), chemistry (i.e., oxic state), and physics (i.e., degree of mixing) of the surrounding water (Richardson et al. 2017). In particular, there is a critical need to better understand controls on ecosystem function along lake shores, as surface and bottom waters may respond at offset timescales to changes in climate (Lewis et al. 2025), and nearshore areas in oligotrophic lakes are displaying visible changes in productivity (i.e., filamentous algal blooms, Vadeboncoeur et al. 2021).

Classification approaches of time series have been used to gain insights into freshwater ecosystem dynamics by identifying unique temporal signatures in salinity (Bolotin et al. 2022), silicon (Johnson et al. 2024), and metabolic regimes in rivers (Savoy et al. 2019). Changes in distinct temporal signatures through space and time can reveal the relative strength of various environmental controls on a solute of interest. With respect to DO, three key parameters characterize diel (i.e., 24 h) time series: (1) mean daily DO, (2) DO amplitude, and (3) the lag between the peak of DO and solar

noon (Odum 1956; Chapra and Di Toro 1991). In the littoral zone of lakes, we expect that mean daily DO is largely controlled by seasonal fluctuations in water temperature that determine DO saturation. While still sensitive to water temperature, we expect the amplitude and lag in the peak of DO relative to solar noon to be more sensitive to differences in productivity, respiration, and gas exchange that vary with depth and proximity to stream inlets (Fig. 1). High gas exchange can dampen the amplitude of DO by keeping DO saturation near 100%, while high biological activity (i.e., photosynthesis and respiration) can increase DO amplitude and cause a greater offset of DO relative to solar noon because of the accumulation of DO in the water column owing to photosynthesis that occurs faster than equilibration with the atmosphere. A question that remains largely unexplored is whether and which diel DO patterns emerge owing to various abiotic and biotic controls in the highly dynamic littoral zone. DO is a reactive solute in freshwater ecosystems that provides insight into biological processes and is, itself, a control on aquatic biogeochemistry. With the advent of high frequency, in situ DO sensors, it has become possible to monitor DO and use it as a tool to measure how aquatic ecosystems may respond to environmental changes.

Across water depths, we hypothesized that shallower sites would receive more light and nutrients from incoming streamflow (Naranjo et al. 2019; Vadeboncoeur et al. 2021) and display heightened biological activity. Shallower sites would therefore have lower mean daily DO values owing to warmer temperatures, as well as greater diel DO amplitudes, and afternoon DO peaks more lagged relative to solar noon (Fig. 1, water depth inset). At deeper sites, we hypothesized that greater light attenuation would decrease biological signals, resulting in dampened DO amplitudes near the lake bottom, but owing to reduced gas exchange, peak DO would still be lagged relative to solar noon. We also hypothesized that these dynamics could shift seasonally, where in summer, high light might cause ultraviolet (UV) photoinhibition of periphyton (Naranjo et al. 2019), and data would display a dampened diel DO amplitude and DO peak more synchronous with solar noon. At sites located near and far from inflowing streams, we hypothesized that DO patterns would converge over the course of data collection as waters warmed and the relative influence of stream discharge abated (Fig. 1, stream discharge inset). We hypothesized that mean daily DO saturation near inflowing streams would be higher in spring owing to the entrainment of cold meltwaters capable of dissolving higher DO concentrations as well as increased gas exchange in steep, mountain streams (Ulseth et al. 2019). We also hypothesized that DO patterns near inflowing streams would display a greater diel amplitude and lag relative to solar noon owing to diel discharge cycles characteristic of snowmelt. As the year progressed, we hypothesized that the diel DO amplitude in summer would

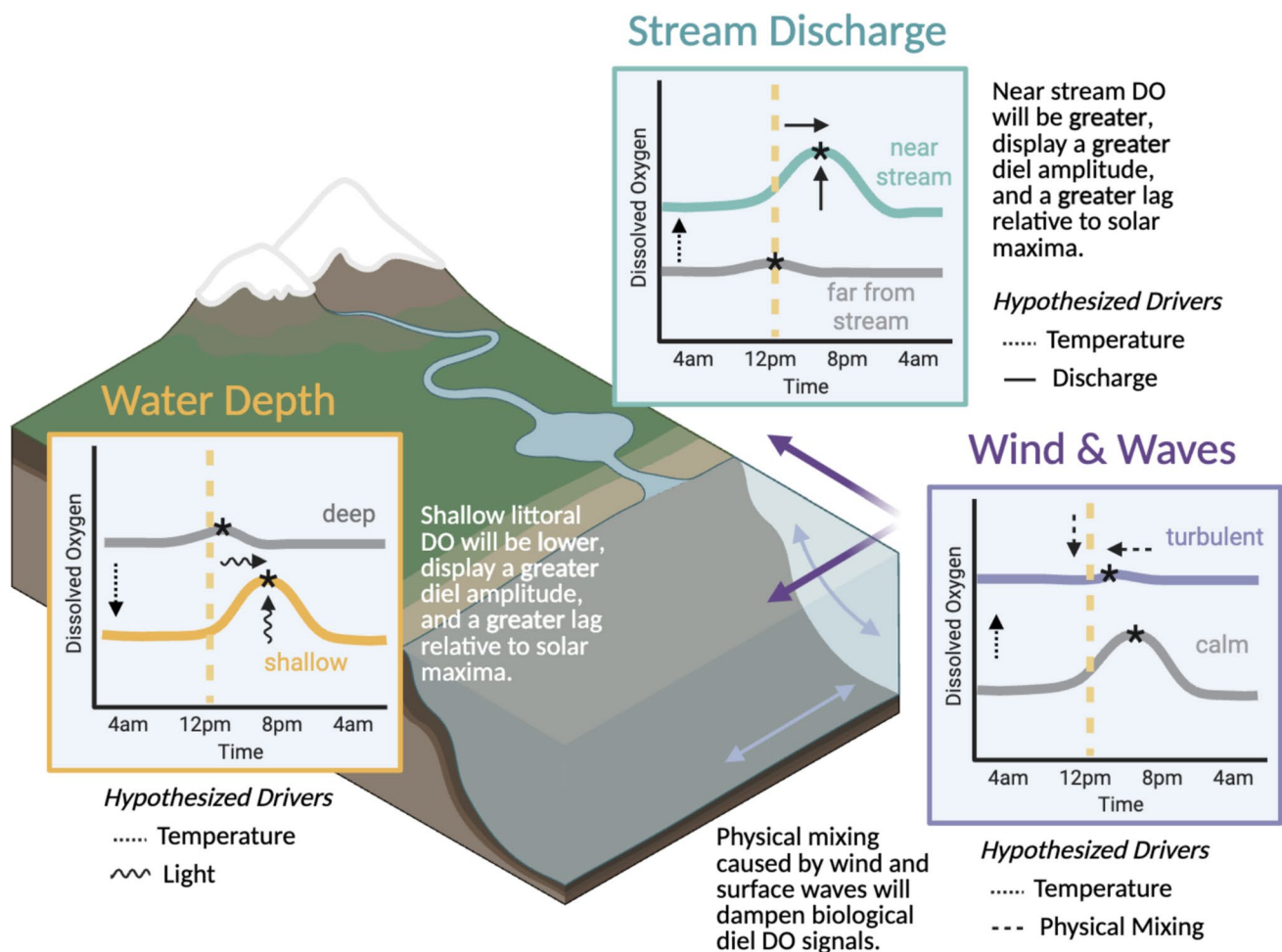


Fig. 1 Hypothesized diagrams of diel dissolved oxygen (DO) patterns responding to environmental drivers; each inset displays two hypothesized DO trajectories when they are (colored) and are not (gray) acted upon by the respective driver. Across a depth gradient, we hypothesized that shallower sites with greater light availability would have lower overall DO owing to warmer waters having a lower dissolution capacity and that a strong photosynthetic signal would increase diel DO amplitude and make diel peaks less synchronous with solar noon (*water depth inset*). To account for watershed DO inputs, we hypothesized that, during spring snowmelt, sites near inflowing streams

would display elevated DO owing to cold meltwaters having a higher dissolution capacity and that a stronger discharge signal that would increase diel DO amplitude and make diel peaks less synchronous with solar noon (*stream discharge inset*). At all sites and during all seasons, we hypothesized that physical mixing would dampen diel DO amplitude but increase the overall magnitude of DO owing to entrainment of colder water; calmer conditions would instead display a stronger diel signal owing to biologically derived oxygen (*wind and waves inset*)

dampen with less snowmelt. In addition to water depth and streamflow, we hypothesized that diel DO amplitude would be dampened by physical mixing owing to wind and surface waves (Fig. 1, wind and waves inset).

This study makes use of DO data measured in the littoral region of an oligotrophic mountain lake (Lake Tahoe, Nevada/California, USA) to examine the relative influence of biological, physical, and watershed drivers on diel and seasonal DO patterns. In the first year of the study, we examine how DO varies as a function of biological and physical controls as mediated by water depth. Instrumentation was deployed as part of a larger stream-to-lake sampling schema that also included sensors in upstream reaches (Loria et al.

2025a). In the second year, we monitored sites at only the shallowest depths located both near and far from inflowing streams to examine how discharge, particularly following spring snowmelt, might affect nearshore littoral DO. Ultimately, our goal was to identify the processes responsible for daily DO patterns in nearshore areas of a large, oligotrophic lake. We examine the influence of local weather and flow conditions in nearshore regions and illustrate the importance of using high-frequency water quality data to inform predictions of how varied abiotic disturbances, such as high variability in snowpack that alters stream discharge (Kapnick et al. 2018), might affect oxygen availability and primary productivity.

Materials and methods

Site description

Lake Tahoe is an oligotrophic mountain lake (1898 m elevation, 505 m maximum depth) located in the Sierra Nevada Mountains (USA; Goldman 1988). The lake does not freeze in winter and is monomictic, although it does not mix to the bottom every year (unstratified period December to May, Roberts et al. 2018). The littoral region in Lake Tahoe, with 1% of surface light reaching maximum littoral depth, typically includes areas < 60 m in depth and represents approximately 19% of the total 500-km² surface area (Goldman 1988; Loeb et al. 1983). In this study, we instrumented four littoral locations (maximum 20 m depth), two on the east shore (inflow from Glenbrook Creek and no perennial discharge at Slaughterhouse Canyon) and two on the west shore (inflow from Blackwood Creek and no perennial discharge at Sunnyside Marina; Fig. 2). Glenbrook Creek drains a steep, 11-km² watershed, which is primarily forested at higher elevations while transitioning into developed areas and wetlands at lower elevation, and empties into the gently sloping Glenbrook Bay. Blackwood Creek drains a gradually sloping, 29-km² watershed, which is primarily undeveloped and forested throughout and empties into a relatively steep littoral region (Coats et al. 2016; Leonard et al. 1979). In addition to contrasting topographies and bathymetries on either shore, Lake Tahoe experiences significant variability in precipitation between the western (mean annual precipitation [MAP] = 140 cm yr⁻¹) and eastern (MAP = 67 cm yr⁻¹) shores (Coats et al. 2008). Most annual precipitation falls as snow, and in the winter of 2022–2023, the region received a record snowfall (> 300% median snow water equivalent as of 1 May 2023; Natural Resources Conservation Service 2024) that has become recognized as a “hydroclimate whiplash” event that transitioned the region from severely dry conditions, marked by drought and wildfires, to severely wet conditions, marked by flooding and landslides (Swain et al. 2025). Additional meteorological information is presented in the Supporting Information.

Data collection and instrument maintenance

During the first stage of data collection from April 2022 through February 2023 (hereafter referred to as stage I), we instrumented two littoral areas near inflowing streams (Fig. 2). We deployed sensors (miniDOT, Precision Measurement Engineering, Inc.) recording dissolved oxygen (DO) concentrations (accuracy = ±5% or ±0.3 mg/L,

whichever is larger) and water temperature (accuracy = ±0.1 °C) at 15-min intervals. Sensors, each paired with a wiper, were oriented in a T-shaped pattern offshore of the Glenbrook Creek (east shore; GB) and Blackwood Creek (west shore; BW) inlets. We deployed three DO sensors parallel to shore in nearshore (NS) littoral areas (approximately 3 m depth). The sensors were attached horizontally to cinder blocks (approximately 0.25 m above the benthos) and placed at 50-m intervals immediately in front of (NS2), north of (NS1), and south of (NS3) inflowing streams to capture potential variation in the inflowing plume of stream discharge. We deployed another three DO sensors perpendicular to shore in shallow littoral (SL, 10 m depth), mid-littoral (ML, 15 m depth), and deep littoral (DL, 20 m depth) locations by securing sensors to a moored buoy line approximately 1 m above the benthos. During stage I, we serviced instruments and downloaded data approximately every 3 months.

During the second stage of data collection from June through September 2023 (hereafter referred to as stage II), we altered the pattern of instrumentation on both shores to monitor ecosystem processes near and far from inflowing streams (Fig. 2). We kept the three sensors deployed in nearshore littoral areas at the inflowing streams in place. We moved sensors from the deeper SL, ML, and DL locations to Slaughterhouse Canyon (SH; approximately 1.2 km north of the Glenbrook Creek inlet) and Sunnyside Marina (SS; approximately 2.8 km north of the Blackwood Creek inlet)—nearshore (NS) littoral regions with no inflowing streams. The new SH and SS deployment locations were selected on the basis of site access and distance relative to other inflowing streams. We were unable to maintain a gradient design as in stage I owing to limited availability of instrumentation. During stage II, we serviced instruments and downloaded data approximately monthly owing to calmer conditions and increased likelihood of biofouling. At the conclusion of the study, we performed a final intercalibration test; for sensors that displayed an offset from anticipated DO values at saturation, we applied an offset correction to the data prior to conducting further analyses. Additional information regarding calibration, maintenance, and the deployment schedule is provided in the Supporting Information (SI). All data are published via the Environmental Data Initiative (Loria et al. 2025b).

Data analyses

In our regression analyses, we combined water depth with incoming light, wind, and stream discharge data. We used these variables to investigate the influence of bathymetry, photosynthesis (made possible by light), gas exchange (facilitated by winds), and watershed inputs (primarily from stream discharge during spring snowmelt) on DO patterns.

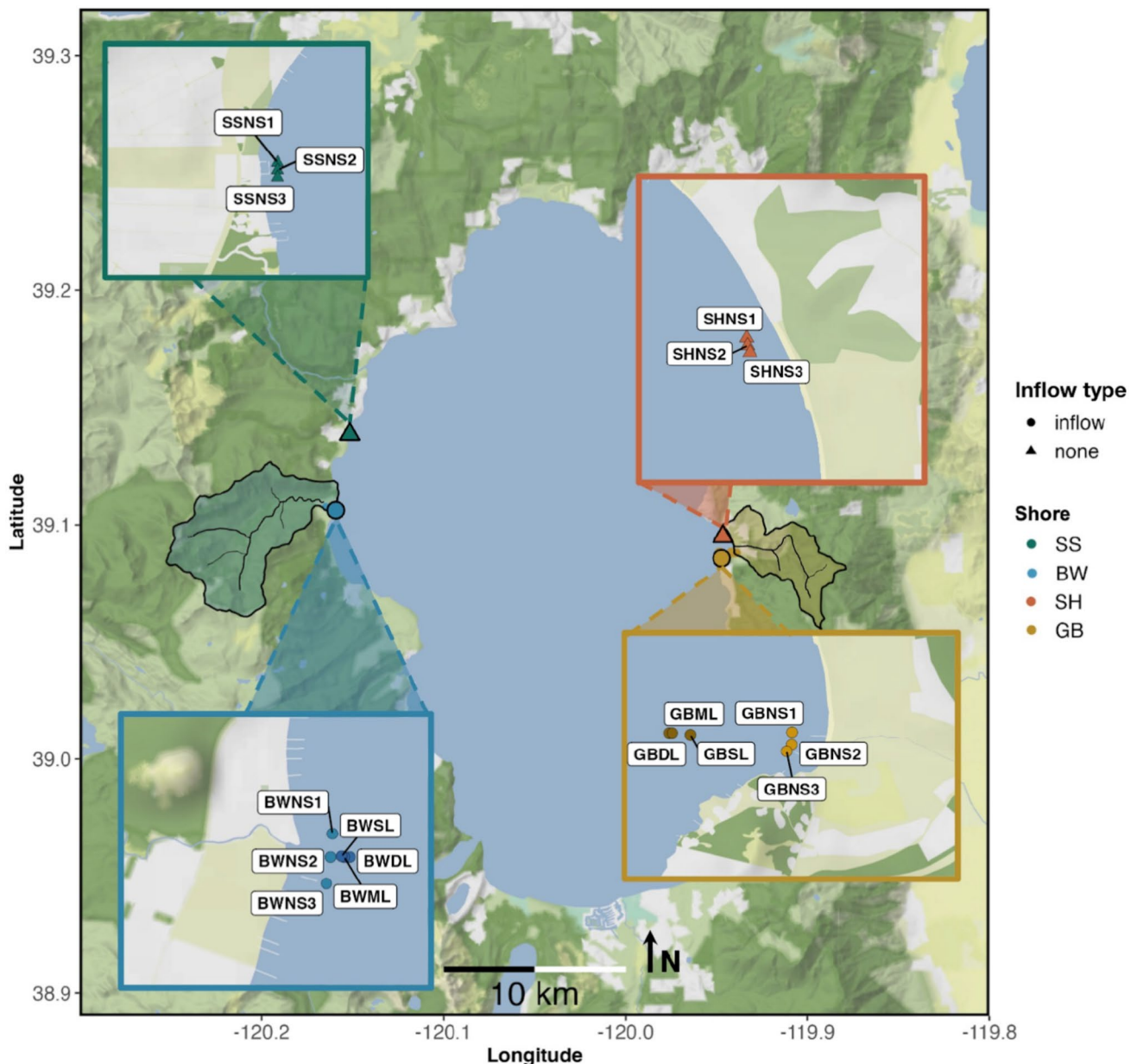


Fig. 2 A map of Lake Tahoe with insets on either shore depicting instrumentation setups. During stage I of this study (April 2022 to February 2023), six dissolved oxygen sensors were deployed on both the east and west shores of Lake Tahoe near Glenbrook (GB) and Blackwood (BW) Creeks, whose watersheds are highlighted in yellow and blue, respectively. Three sensors were deployed in nearshore (NS) littoral locations parallel to shore at 50-m intervals immediately in front of (NS2), north (NS1), and south (NS3) of inflowing streams, and another three were deployed perpendicular to shore in shallow lit-

toral (SL, 10 m depth), mid-littoral (ML, 15 m depth), and deep littoral (DL, 20 m depth) locations. During stage II of this study (June to September 2023), the three sensors deployed parallel to shore in front of inflowing streams were left in place. The remaining three sensors were moved to a northern location further from an inflowing stream, Slaughterhouse Canyon (SH) on the east shore and Sunnyside Marina (SS) on the west shore, and deployed in nearshore (NS) littoral locations parallel to shore at 50-m intervals with central (NS2), northern (NS1), and southern (NS3) locations

To gather these data, we downloaded incoming light (hourly shortwave radiation flux in W m^{-2}) and wind data (every 3 h in m s^{-1}) from the North American Land Data Assimilation System (Xia et al. 2012; refer to the SI for details); we chose to use these gridded data products rather than local

meteorological stations' data owing to the latter not being available at all sites and displaying interferences from local canopy and hillshade. We downloaded mean daily stream discharge (parameter code 00060, $\text{ft}^3 \text{s}^{-1}$) using the US Geological Survey's *dataRetrieval* R package (De Cicco

et al. 2024) for both Glenbrook (site code: 10,336,730) and Blackwood Creeks (site code: 10,336,660). We chose not to impute or interpolate missing covariate data and instead removed those days from our analysis. Additional details regarding environmental covariate data collection and preparation are detailed in Loria et al. (2025a).

We determined dominant diel patterns in littoral DO using dynamic time-warping (DTW, Sardá-Espinosa 2019). Initial efforts to estimate metabolism (i.e., gross primary production and ecosystem respiration) yielded poor model fits, and DTW provides an alternative method to classify daily data on the basis of time series' trajectories. The DTW approach compares two time series on the same plane and determines a warping path that best minimizes the distance measure between their two paths (Berndt and Clifford 1994; Sakoe and Chiba 1978). Following all pairwise comparisons and using computed distance measures, time series may be clustered into groups to identify the dominant patterns. We used fuzzy *c*-medoids clustering to allow for the creation of multiple, overlapping groups where each time series is allowed partial membership in multiple groups (Izakian et al. 2015). DTW is well suited for examining ecosystem phenology, which often necessitates elastic rather than 1:1 methods of comparison (Savoy et al. 2019).

Prior to fitting the DTW model, we filtered DO data to remove days of deployment/retrieval, instrument malfunction, and suspected biofouling (additional quality assurance and quality control [QA/QC] details available in the SI). To aggregate data at a daily time-step, we split mean hourly data between stage I and stage II periods and divided it again into 24-h-long time series beginning at 04:00 (before sunrise). We further *z*-score-normalized all data (i.e., subtracted the mean value and divided by the standard deviation of all DO values). We then fit DO (% saturation) time series using the *tsclust* function (type = "fuzzy", centroid = "fcmdd") in the *dtwclust* R package (Sardá-Espinosa 2019) using R version 4.4.1 (R Core Team 2024). To improve model convergence, we constrained the warping window size to 3 h and ran the model for 1000 iterations. We examined 2–12 cluster options and identified the model fit that was best supported by a majority of five internal, fuzzy cluster validity indices (Sardá-Espinosa 2019; Wang and Zhang 2007). Following the selection of the model with the number of clusters best supported by the validity indices (refer to the SI for more details), cluster membership was determined for each day's DO pattern using a 90% threshold; if a day's data did not achieve higher than 90% membership for any of the possible clusters it was assigned to a "no cluster membership" category. We additionally fit time series for raw DO data (mg/L), the full results of which are provided in the SI (Supplementary Figs. S15, S16).

To quantify relationships between environmental controls and cluster membership, we fit two Bayesian multilevel,

multinomial logistic regression models, one for each stage of the project. We removed strongly correlated covariates (Pearson's $r > 0.7$), log-transformed stream discharge, and *z*-score-normalized all continuous, numerical covariates. For stage I ($n = 2770$ days), the final model structure included water depth, cumulative daily light, mean daily wind speed, and mean daily stream discharge as individual covariates to investigate the influence of bathymetry, climate, gas exchange/mixing, and watershed inputs on cluster membership. For stage II ($n = 821$ days), we removed water depth as a covariate since all sensors were at the same depth. In both models, a nested, group-level intercept of site (BW, GB, SS, SH) and individual sensor ID were included to account for repeated sampling (i.e., non-independent samples) and the potential effects of site-specific conditions. We investigated numerous potential covariates and detail our justification for the final model structure here. Cumulative daily light, rather than day length, was chosen to represent climate and light availability since these two terms were found to be strongly correlated throughout the study (Supplementary Fig. S21). Minimum DO (% saturation) values were examined as a potential covariate indicative of respiration but aligned closely with the group level curves (Supplementary Fig. S22) and therefore were not included. We also fit the model structure including an autoregressive (AR[1]) term but found that it overwhelmed all other covariates included (Supplementary Fig. S23) and therefore did not include it. Finally, we chose not to include lake shore as a covariate because it was highly correlated with water depth (owing to instrument malfunctions) during stage I and stream discharge (owing to stream size) during stage II; lake shore was also not included as an interacting covariate owing to concerns of estimating too many parameters and making model interpretability challenging (Supplementary Fig. S24).

We fit models in a Bayesian framework using the *brms* package (Bürkner 2017), with four chains run for 2000 iterations each with 1000 warm-up iterations (i.e., 4000 total iterations). We visually inspected for good chain mixing and a lack of divergent transitions, and we ensured a Gelman–Rubin statistic (\hat{R}) < 1.05 and an effective sample size $> 10\%$ for all parameters. We extracted median posterior values and 95% credible intervals using the *tidybayes* package (Kay 2024). Posterior predictive figures are included in the SI. In addition, we used the results of the raw DO data clustering to fit models that included water temperature along with the covariates listed above for both stages of the project; the full results are shown in the SI (Supplementary Figs. S17, S18, S19, S20). We included temperature as a predictor only in these regression models because we did not feel that it was appropriate to include temperature in a model where % DO saturation had been calculated using those same data.

Results

Across the littoral depth gradient (stage I), two seasonal clusters emerged that showed increased DO saturation values coupled to greater lags in peak values relative to solar maxima (Fig. 3). In total, 27% of days were grouped in

the “synchronous” cluster, 30% of days were grouped in the “lagged” cluster, and 42% of days were not assigned to either cluster (Fig. 3a, Table 1). Cluster peaks both lagged maximum incoming light, with the “synchronous” cluster less offset than the “lagged” cluster. The earlier-peaking, “synchronous” cluster had lower daily DO than the “lagged” cluster; amplitudes of the diel DO patterns (i.e.,

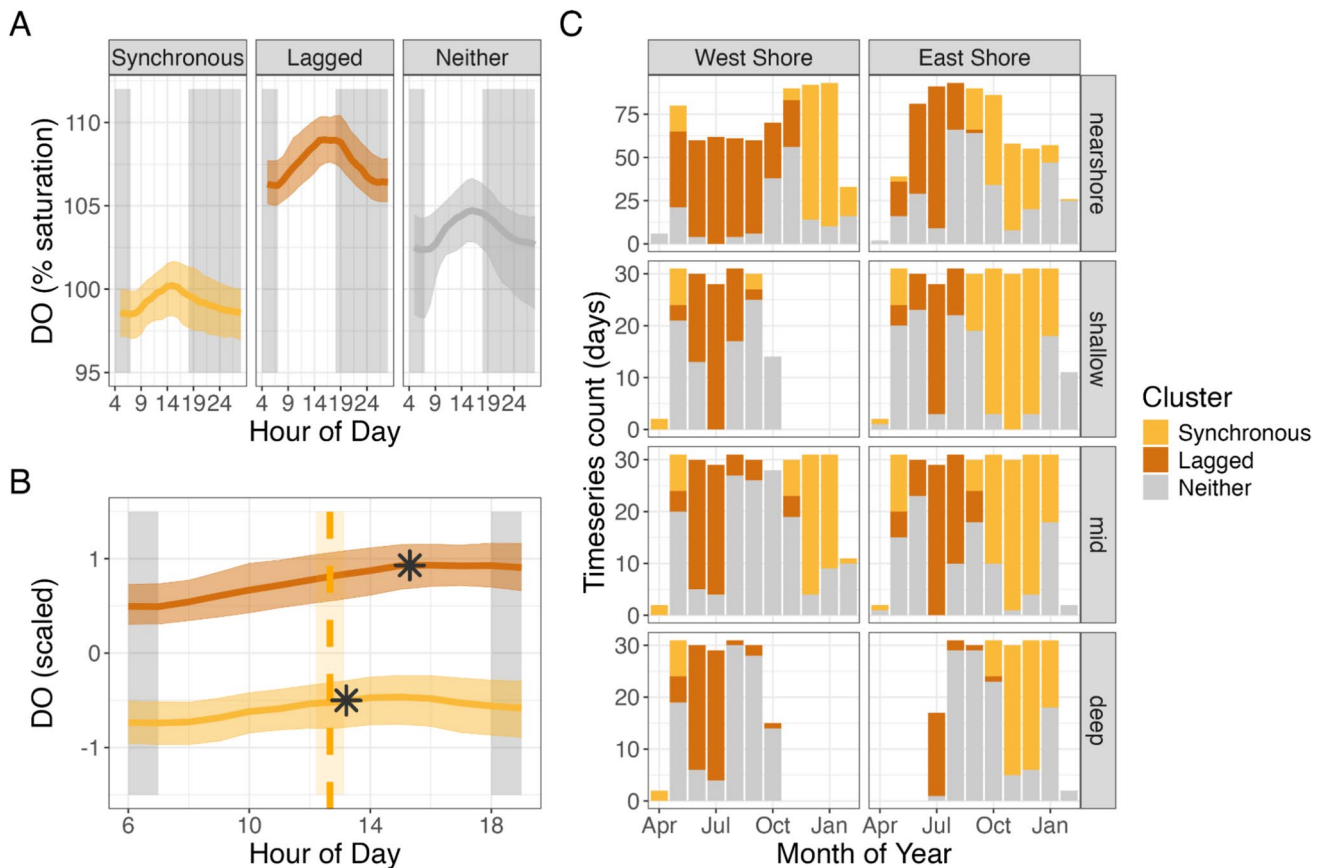


Fig. 3 Median diel time series for littoral zones of Lake Tahoe, California/Nevada, represented as **A** dissolved oxygen percent saturation and **B** z-score-normalized values from stage I (April 2022 to February 2023) according to the dynamic time-warping (DTW) cluster that they most belong to (>90%). Shading around each curve denotes the 25th and 75th percentiles. Gray, boxed shading denotes approximate

mean annual daily hours of darkness. In panel B, the dashed line is the mean annual solar noon (orange shading denotes ± 1 s.d.), and the stars indicate the mean hour of dissolved oxygen (DO) maxima for each cluster. **C** The number of days that belong to each cluster according to lake shore (west, east), water depth (nearshore littoral, shallow littoral, mid-littoral, deep littoral), and month of the year

Table 1 Attributes of clusters of diel dissolved oxygen (DO) patterns identified by the dynamic time-warping approach for stage I (April 2022 to February 2023). DO amplitude was calculated as the difference between daily maximum and minimum values

Stage I (depth) clusters	Mean daily DO (% saturation) mean \pm s.d	Mean daily DO amplitude (% saturation) mean \pm s.d	Time offset of solar maxima (min) mean \pm s.d
Synchronous (n = 758)	99.06% \pm 1.78%	3.27% \pm 2.58%	58 \pm 274
Lagged (n = 836)	107.7% \pm 1.61%	4.95% \pm 3.39%	138 \pm 210
Neither (n = 1176)	102.5% \pm 7.12%	6.87% \pm 8.93%	73 \pm 289

maximum daily DO – minimum daily DO) were similar across clusters (Fig. 3b, Table 1).

Clusters were distinctly seasonal, with the “lagged” cluster the most prevalent in summer months (May to September) and the “synchronous” cluster more common during the remaining months of the year (Fig. 3c). The “synchronous” cluster also appeared more frequently on the east shore, although this may be in part owing to lack of data at deeper depths on the west shore (data were removed owing to suspected biofouling). In addition to DO pattern attributes, days in the “synchronous” cluster displayed a lower mean daily water temperature (9.1 ± 3.9 °C) and a smaller mean daily range in water temperature (0.8 ± 0.6 °C) than days in the “lagged” cluster (mean daily temperature = 14.7 ± 3.9 °C, mean daily range = 1.8 ± 1.1 °C).

At nearshore sites near and far from inflowing streams (stage II), two clusters emerged, largely on opposite shores, that showed increased DO saturation values coupled with

smaller lags in peak values relative to solar maxima (Fig. 4). A total of 29% of days were grouped in the “synchronous” cluster, 27% of days were grouped in the “lagged” cluster, and 44% of days were not assigned to either cluster (Fig. 4a, Table 2). Cluster peaks both lagged maximum incoming light, with the “lagged” cluster more offset than the “synchronous” cluster. The later-peaking, “lagged” cluster had a lower mean daily DO than the “synchronous” cluster; amplitudes of the diel DO patterns were again not distinguishable across clusters (Fig. 4b, Table 2).

Clusters appeared distinct by shore, with the “lagged” cluster more frequent on the east shore and the “synchronous” cluster on the west shore. Seasonality of clusters was less evident during this stage of the project, although the east shore did appear to transition from more instances of the “synchronous” to the “lagged” cluster over the course of the summer season (Fig. 4c). In addition to DO pattern attributes, days in the “lagged” cluster displayed a higher mean

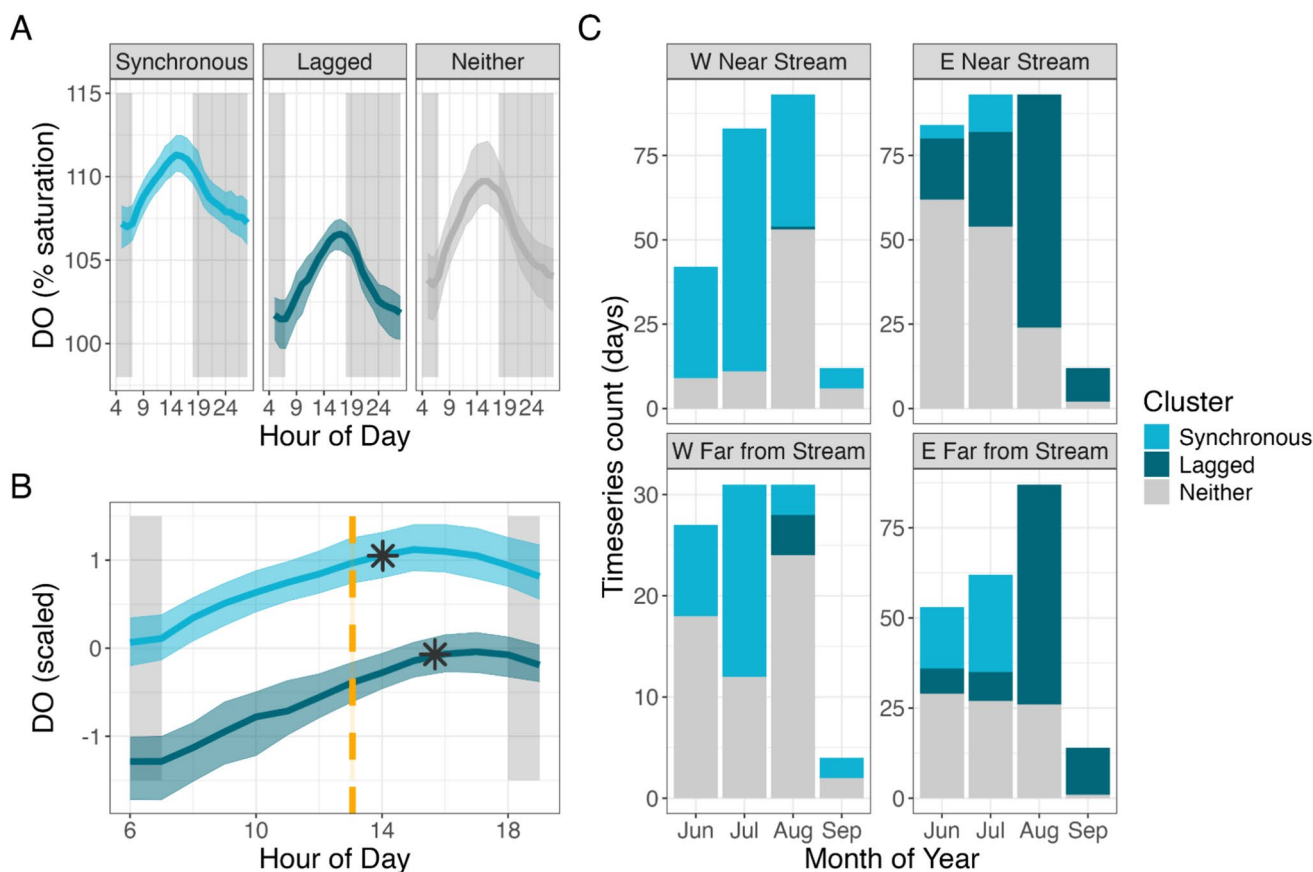


Fig. 4 Median diel time series for nearshore littoral zones of Lake Tahoe, California/Nevada, represented as **A** dissolved oxygen percent saturation and **B** z-score-normalized values from stage II (June to September 2023) according to the dynamic time-warping (DTW) cluster that they most belong to (>90%). Shading around each curve denotes the 25th and 75th percentiles. Gray, boxed shading denotes approximate mean annual daily hours of darkness. In panel

B, the dashed line is the mean seasonal solar noon (orange shading denotes ± 1 s.d.), and the stars indicate the mean hour of dissolved oxygen (DO) maxima for each cluster. **C** The number of days that belong to each identified cluster according to lake shore (east or west), distance from inflowing stream (near or far), and month of the year. Note, all instruments during stage II were placed in the nearshore littoral zone (approximately 3 m water depth)

Table 2 Attributes of clusters of diel dissolved oxygen (DO) patterns identified by the dynamic time-warping approach for stage II (June to September 2023). DO amplitude was calculated as the difference between daily maximum and minimum values

Stage II (stream proximity) clusters	Mean daily DO (% saturation) mean ± s.d	Mean daily DO amplitude (% saturation) mean ± s.d	Time offset of solar maxima (min) mean ± s.d
Synchronous (n = 242)	109.18% ± 0.98%	6.66% ± 2.55%	57 ± 209
Lagged (n = 219)	103.65% ± 1.08%	7.24% ± 3.05%	158 ± 128
Neither (n = 360)	106.95% ± 3.00%	10.29% ± 4.85%	125 ± 189

daily water temperature (19.1 ± 1.9 °C) and a smaller mean daily range (1.1 ± 0.8 °C) than days in the “synchronous” cluster (mean daily temperature = 16.6 ± 2.7 °C, mean daily range = 2.3 ± 1.4 °C).

In contrast to the DTW results for DO saturation patterns, results for DO concentration patterns were distinguished only by overall magnitude of the diel DO patterns, not by amplitude or timing of peaks; low DO concentration clusters appeared exclusively in late summer and early fall (July to October) during both stages of the project (Supplementary Figs. S15, S16). It follows that water temperature was the overwhelming predictor of raw DO concentration patterns (Supplementary Fig. S17). These results support our focus on DO saturation values, as DO concentration appears driven by seasonal water temperatures.

Across the entire study, light availability and stream discharge had the strongest effects on DO saturation cluster membership (Fig. 5). For stage I, the “synchronous” cluster days occurred on days with lower light (i.e., cumulative daily light availability; $\beta_{\text{light}} = -1.33$, credible interval (CI)₉₅ = [-1.49, -1.18]) and higher stream discharge (i.e., mean daily discharge; $\beta_{\log(Q)} = 0.90$, CI₉₅ = [0.71, 1.10]). The “lagged” cluster days occurred on days with higher light ($\beta_{\text{light}} = 2.02$, CI₉₅ = [1.81, 2.27]), lower stream discharge ($\beta_{\log(Q)} = -0.68$, CI₉₅ = [-0.87, -0.48]), and higher wind (i.e., mean daily wind speed; $\beta_{\text{wind}} = 0.18$, CI₉₅ = [0.05, 0.32]). Water depth did not have a strong effect on cluster membership. During stage II, the “lagged” cluster days occurred on days with lower stream discharge ($\beta_{\log(Q)} = -3.88$, CI₉₅ = [-5.53, -2.37]), lower light

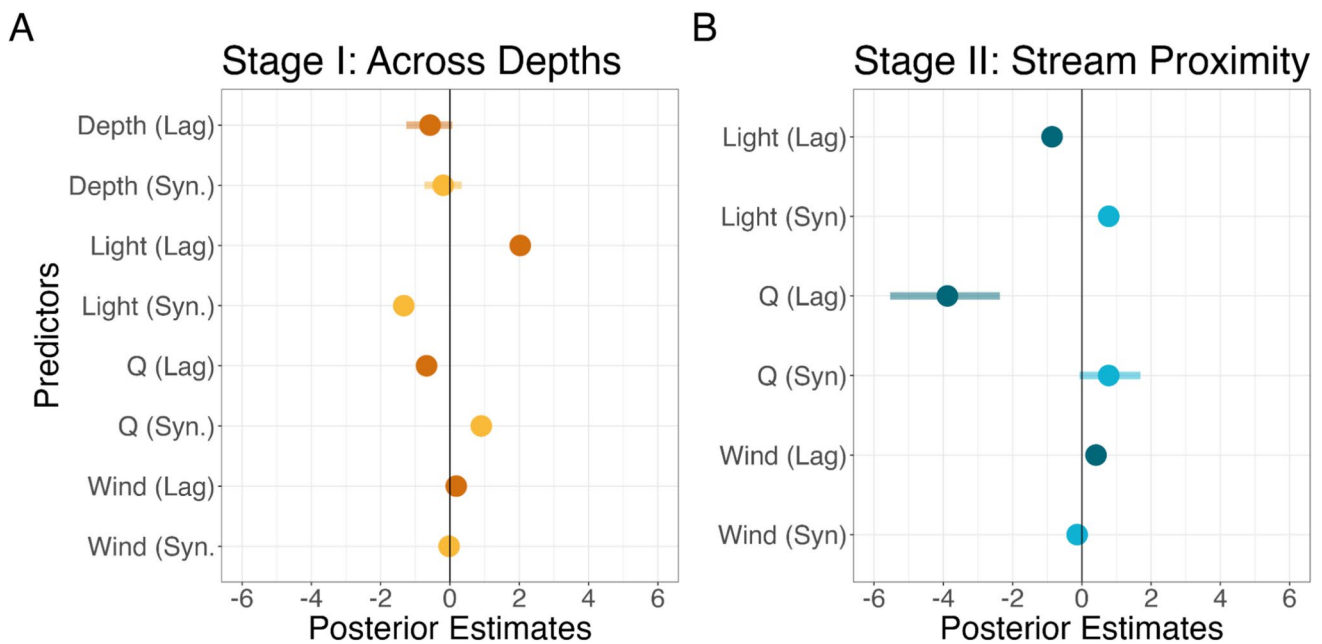


Fig. 5 Results of Bayesian multinomial logistic regressions for **A** stage I (across depths) and **B** stage II (near and far from stream inlets) for littoral zones in Lake Tahoe, California/Nevada. Potential covariates for the daily clustering include water depth (depth), cumulative daily light availability (light), mean daily discharge (Q), and mean

daily wind speed (wind). Points represent median log-odds parameter estimates with shaded lines to denote 95% credible intervals; credible intervals are smaller than the point size when not visible. Coloration of “synchronous” (syn.) and “lagged” (lag) clusters corresponds to Figs. 3 and 4

($\beta_{\text{light}} = -0.86$, $\text{CI}_{95} = [-1.11, -0.62]$), and higher wind ($\beta_{\text{wind}} = 0.41$, $\text{CI}_{95} = [0.20, 0.62]$). The “synchronous” cluster corresponded most strongly with higher light ($\beta_{\text{light}} = 0.78$, $\text{CI}_{95} = [0.51, 1.05]$).

Discussion

We found light availability and stream discharge were strongly correlated with daily dissolved oxygen saturation (hereafter “DO”) patterns in littoral regions of Lake Tahoe, highlighting how both climate and local conditions likely play a strong role in diel DO variation in shallow areas. The DO pattern whose daily peak was more synchronous with solar noon occurred more frequently in late spring, autumn, and winter, when light availability is lower, and during periods of high stream discharge, when littoral regions are more readily linked to the surrounding watershed via water and material transport. In contrast, the “lagged” daily DO pattern occurred nearly exclusively in summer and more frequently during periods (or at locations) of lower stream discharge, suggesting a heightened importance of within-lake processes and a relative decoupling from climate (i.e., light) or watershed (i.e., streamflow) inputs on these days. Together, these data support the idea that the littoral zone is a “sentinel-of-the-sentinel” (Ward et al. 2022), displaying rapid, detectable changes in water quality and ecosystem function in response to climate and physical conditions.

While sensors were deployed along a depth gradient (stage I), a seasonal signal dominated variation in DO patterns; clusters were positively correlated with light availability in summer and stream discharge in winter and spring. We initially hypothesized that diel DO patterns indicative of biology (i.e., photosynthesis, Fig. 1) would emerge at shallower sites. We did find a positive relationship between daily cumulative light and the “lagged” cluster (Fig. 5a) but the pattern emerged across all water depths, not only at shallow sites. This suggests that the greatest primary productivity signal is coupled with the highest light availability in summer, which is in contrast to Naranjo et al. (2019) who found productivity of littoral periphyton in Lake Tahoe to be greater in winter and spring, when nutrients are abundant but solar radiation has not reached levels capable of photoinhibition (Huovinen and Goldman 2000). We instead found that in fall, winter, and spring, the “synchronous” cluster whose peak was closer to solar noon was most common (Fig. 3b). We propose that the significant precipitation and winter storm activity of late 2022 and early 2023 may be responsible for why we see little evidence for photosynthetic activity outside of the summer season and why mean daily DO and daily amplitude decreased substantially across all depths.

We investigated how DO patterns changed with depth in response to inflowing streams across two different shoreline

bathymetries (i.e., steep declines in depth on the west shore and a shallow bay on the east shore), yet we detected no effect of depth on DO saturation patterns. We further hypothesized that DO patterns characteristic of physical processes (e.g., dampened daily amplitude, Fig. 1) would display a strong relationship with wind but found no relationship between mean daily wind and the lower DO amplitude pattern (the “synchronous” cluster, Fig. 5a). Because cluster membership was strongly correlated with daily stream discharge (Fig. 5a), we propose that discharge from Glenbrook and Blackwood Creeks created greater variability by season and may have obscured our observation of a depth gradient in littoral DO saturation patterns. Other studies located in lotic-to-lentic transition zones have reported that the depth of stream inflow into a lake may vary significantly as a function of stream water temperature (Ward et al. 2022) as well as the degree of stratification in the recipient waterbody (Cortés et al. 2014a). We recommend future work conducted in littoral zones of lakes strongly consider periods during or locations in which the stream–lake transition zone is strongly coupled and to what degree this may influence the ability to detect variability between sites.

When considering only nearshore littoral sites (3 m depth; stage II), we detected greater differences in DO patterns across shores rather than near and far from streams. We initially hypothesized that sites nearest streams would display distinct DO signals (i.e., peaks offset of solar maxima due to stream inflows). However, we found that the later-peaking DO pattern appeared most on the east shore (the “lagged” cluster, Fig. 4) and was correlated with lower discharge (Fig. 5b). Glenbrook Creek, the smaller stream on the east shore, drains a small, steep watershed, and in Lake Tahoe, the influence of stream discharge on nearshore littoral productivity has been shown to scale with catchment size, with greater stream inflows creating more heterotrophic conditions in nearshore areas (Loria et al. 2025a). Together, these findings suggest that Glenbrook Creek’s more rapid return to base flow conditions during summer 2023 (Loria et al., *in revision*) and a wider, shallower bathymetry may have stimulated more productivity (i.e., more autotrophic conditions) and thereby more lagged DO patterns. We further posit that physical mixing owing to high discharge following the multiple storms and record snowfall in 2023 (Natural Resources Conservation Service 2024; Swain et al. 2025) likely made differences between sites near and far from streams more muted. These patterns highlight how heterogeneous lake shores can be and the need for better characterization of multiple locations when investigating littoral zones within lakes.

In this study, clustering via a dynamic time-warping (DTW) technique enabled us to identify distinct patterns in daily DO in an oligotrophic system in which traditional metabolism modeling approaches were not suitable. The two clusters that were identified in both stages of the project

were strongly supported by a suite of cluster validity indices, and therefore we feel confident in the number of clusters retained as descriptive of generalized daily DO trajectories. However, we acknowledge that the DTW method possesses particular challenges and address several of them here for others interested in this approach. First, DTW is a classification method intended to facilitate simpler comparison of complex time series and does so by identifying common trajectories across multiple sets of observations. If researchers are focused instead on the detection of rare or short-lived anomalies in their data, this approach may not be suitable for detecting more nuanced signals. In addition, DTW outputs may be challenging to interpret if not properly informed by the model system. We advise those using DTW to document hypothesized trajectories prior to fitting the model to aid with interpretation of the resulting clusters. This will also inform a key decision—the threshold of cluster membership required for a set of observations to be assigned to a particular cluster. We chose a 90% threshold of belonging, as others have done (Bolotin et al. 2022), because we sought to maximize the likelihood of identifying potential environmental drivers for a given cluster. Many of our days did not meet that threshold and belong to neither cluster, but we were able to detect strong correlations with environmental factors (i.e., light and discharge) among the two primary clusters and therefore feel this was an appropriate threshold. Although we do not explore this application, the results of DTW clustering may also be used to examine trajectories upon trajectories or how an ecosystem moves among groups (Savoy et al. 2019). Others have begun to observe how rivers, for example, transition between silica regimes (Johnson et al. 2024), but there remain exciting opportunities to apply this approach in the context of ecosystem resistance and resilience to disturbance.

Our analyses of data collected from sensors in littoral regions of Lake Tahoe were able to examine relationships between DO patterns and environmental conditions in a highly oxygenated, low-productivity lake. Higher DO saturation patterns (i.e., greater mean daily values) were consistently correlated with higher light availability, creating strong seasonality in littoral DO. With increasing instances of summer wildfires, lakes are more frequently subject to smoke effects, which could alter this seasonality by decreasing incoming solar radiation (Farruggia et al. 2024) and increasing pelagic productivity relative to littoral sites (Scordo et al. 2022). Stream discharge also emerged as an important factor, which has significant implications given the predicted declines (Kapnick et al. 2018) and variability in melt dynamics of western snowpacks (Koshkin et al. 2022). At the global scale, lake temperatures are warming (Williamson et al. 2009; Woolway et al. 2020), which poses a threat to shallow regions that may warm more rapidly and experience lower DO

solubility and deoxygenation (Jane et al. 2021). Instances of filamentous algal blooms are also becoming more frequent in nearshore regions of oligotrophic lakes (Vadeboncoeur et al. 2021), which could lead to large diel swings in DO during the bloom followed by consumption of DO owing to respiration following the bloom. As lakes display considerable spatial variability in timescales of response to climate change (Lewis et al. 2025), all of these aforementioned factors—fire, snow, streamflow, warming, algal blooms—will likely yield a mosaic of responses across littoral, pelagic, and benthic regions. To better interpret data collected via a network of sensor deployments, we must develop a better understanding of the possible spatial differences in DO and posit that this study provides a novel way to analyze diel DO patterns and a reference for how such patterns in the littoral zones of lakes could be interpreted. Ultimately, additional work is needed to understand how increasingly variable climate and watershed inputs determine the spatial and temporal heterogeneity of littoral water quality (i.e., temperature and oxygen availability) and ecosystem function.

Supplementary Information The online version contains supplementary material available at <https://doi.org/10.1007/s00027-026-01292-5>.

Acknowledgements We thank Zachary Bess, Emily Carlson, Elizabeth Everest, Monique Rydel Fortner, Seth Jones, Rob Miller, Emma Radulovic, and Erin Suenega for their invaluable field, boat, and SCUBA diving assistance as well as Wubneh Belete Abebe, Ian Halterman, Helen Lei, Meredith Brehob, Taryn Elliott, Keenan Seto, and Rija Masroor for laboratory assistance. We also thank the Tahoe Regional Planning Agency and the residents of Glenbrook, Nevada, especially Gary and Susan Clemons, for access to the sites. We thank Alicia Cortés for her assistance with data interpretation and project narrative refinement and Adrienne Smits and Spencer Tassone for helpful edits to the manuscript during the US Geological Survey's internal review process. Financial support for this project was provided by the Nevada Department of State Lands and the National Science Foundation (award no. OIA-2019528 and a Graduate Research Fellowship awarded to K. Loria). Any use of trade, firm, or product names is for descriptive purposes only and does not imply endorsement by the US Government.

Author contributions Conceptualization, funding acquisition, and resources: Heili E. Lowman, Kelly Loria, Sudeep Chandra, and Joanna R. Blaszczyk; Methodology: Heili E. Lowman, Kelly Loria, Leon Katona, Jasmine Krause, and Joanna R. Blaszczyk; Formal analysis and investigation: Heili E. Lowman and Kelly Loria; Writing—original draft preparation: Heili E. Lowman, Kelly Loria, and Joanna R. Blaszczyk; Writing—review and editing: Heili E. Lowman, Kelly Loria, Leon Katona, Jasmine Krause, Sudeep Chandra, Sally MacIntyre, John M. Melack, Ramon Naranjo, and Joanna R. Blaszczyk; Supervision: Joanna R. Blaszczyk.

Funding National Science Foundation, Graduate Research Fellowship, #OIA-2019528, Nevada Department of State Lands

Data availability All data collected by the authors are published via the Environmental Data Initiative. R scripts used to perform the analyses and generate the figures for this manuscript are publicly available at [<https://doi.org/10.5281/zenodo.19320392>] (<https://doi.org/10.5281/zenodo.19320392>).

Declarations

Conflict of interest The authors declare no competing interests.

References

- Berndt, D.J., Clifford, J., 1994. Using dynamic time warping to find patterns in time series. AAAI Technical Report WS-94-03. <https://www.aaai.org/Papers/Workshops/1994/WS-94-03/WS94-03-031.pdf>.
- Bolotin LA, Summers BM, Savoy P, Blaszcak JR (2022) Classifying freshwater salinity regimes in central and western US streams and rivers. *Limnol Oceanogr Lett* 8:103–111. <https://doi.org/10.1002/lo2.10251>
- Bürkner P-C (2017) Brms: an R package for Bayesian multilevel models using Stan. *J Stat Softw* 80:1–28. <https://doi.org/10.18637/jss.v080.i01>
- Chapra SC, Di Toro DM (1991) Delta method for estimating primary production, respiration, and reaeration in streams. *J Environ Eng* 117:640–655. [https://doi.org/10.1061/\(ASCE\)0733-9372\(1991\)117:5\(640\)](https://doi.org/10.1061/(ASCE)0733-9372(1991)117:5(640))
- De Cicco, L.A., Lorenz, D., Hirsch, R.M., Watkins, W., Johnson, M., 2024. dataRetrieval: R packages for discovering and retrieving water data available from U.S. federal hydrologic web services, v.2.7.17. <https://doi-usgs.github.io/dataRetrieval/>.
- Coats R, Larsen M, Heyvaert A, Thomas J, Luck M, Reuter J (2008) Nutrient and sediment production, watershed characteristics, and land use in the Tahoe Basin, California-Nevada. *J Am Water Resour Assoc* 44:754–770. <https://doi.org/10.1111/j.1752-1688.2008.00203.x>
- Coats R, Lewis J, Alvarez N, Arneson P (2016) Temporal and spatial trends in nutrient and sediment loading to Lake Tahoe, California-Nevada, USA. *J Am Water Resour Assoc* 52:1347–1365. <https://doi.org/10.1111/1752-1688.12461>
- Cortés A, Fleenor WE, Wells MG, De Vicente I, Rueda FJ (2014a) Pathways of river water to the surface layers of stratified reservoirs. *Limnol Oceanogr* 59:233–250. <https://doi.org/10.4319/lo.2014.59.1.0233>
- Cortés A, Rueda FJ, Wells MG (2014b) Experimental observations of the splitting of a gravity current at a density step in a stratified water body. *J Geophys Res Oceans* 119:1038–1053. <https://doi.org/10.1002/2013JC009304>
- Farruggia MJ, Brahney J, Tanentzap AJ, Brentrup JA, Brighenti LS, Chandra S, Cortés A, Fernandez RL, Fischer JM, Forrest AL, Jin Y, Larrieu K, McCullough IM, Oleksy IA, Pilla RM, Rusak JA, Scordo F, Smits AP, Symons CC, Tang M, Woodman SG, Sadro S (2024) Wildfire smoke impacts lake ecosystems. *Glob Chang Biol* 30:e17367. <https://doi.org/10.1111/gcb.17367>
- Goldman CR (1988) Primary productivity, nutrients, and transparency during the early onset of eutrophication in ultra-oligotrophic Lake Tahoe, California-Nevada. *Limnol Oceanogr* 33:1321–1333. <https://doi.org/10.4319/lo.1988.33.6.1321>
- Huovinen PS, Goldman CR (2000) Inhibition of phytoplankton production by UV-B radiation in clear subalpine Lake Tahoe, California-Nevada. *SIL Proc* 27:157–160. <https://doi.org/10.1080/03680770.1998.11901217>
- Izakian H, Pedrycz W, Jamal I (2015) Fuzzy clustering of time series data using dynamic time warping distance. *Eng Appl Artif Intell* 39:235–244. <https://doi.org/10.1016/j.engappai.2014.12.015>
- Jane SF, Hansen GJA, Kraemer BM, Leavitt PR, Mincer JL, North RL, Pilla RM, Stetler JT, Williamson CE, Woolway RI, Arvola L, Chandra S, DeGasperi CL, Diemer L, Dunalska J, Erina O, Flaim G, Grossart H-P, Hambright KD, Hein C, Hejzlar J, Janus LL, Jenny J-P, Jones JR, Knoll LB, Leoni B, Mackay E, Matsuzaki S-IS, McBride C, Müller-Navarra DC, Paterson AM, Pierson D, Rogora M, Rusak JA, Sadro S, Saulnier-Talbot E, Schmid M, Sommaruga R, Thiery W, Verburg P, Weathers KC, Weyhenmeyer GA, Yokota K, Rose KC (2021) Widespread deoxygenation of temperate lakes. *Nature* 594:66–70. <https://doi.org/10.1038/s41586-021-03550-y>
- Jankowski KJ, Mejia FH, Blaszcak JR, Holtgrieve GW (2021) Aquatic ecosystem metabolism as a tool in environmental management. *Wires Water*. <https://doi.org/10.1002/wat2.1521>
- Johnson K, Jankowski KJ, Carey J, Lyon NJ, McDowell WH, Shogren A, Wymore A, Sethna L, Wollheim WM, Poste AE, Kortelainen P, Heindel R, Laudon H, Rääke A, Jones JB, McKnight D, Julian P, Bush S, Sullivan PL (2024) Establishing fluvial silicon regimes and their stability across the Northern Hemisphere. *Limnol Oceanogr Letters* 9:237–246. <https://doi.org/10.1002/lo2.10372>
- Kapnick, S.B., Yang, X., Vecchi, G.A., Delworth, T.L., Gudgel, R., Malyshev, S., Milly, P.C.D., Shevliakova, E., Underwood, S., Margulis, S.A., 2018. Potential for western US seasonal snowpack prediction. *Proceedings of the National Academy of Sciences* 115: 1180–1185. <https://doi.org/10.1073/pnas.1716760115>.
- Kay, M., 2024. tidybayes: Tidy data and geoms for Bayesian models, v.3.0.7
- Kirchner JW, Godsey SE, Solomon M, Osterhuber R, McConnell JR, Penna D (2020) The pulse of a montane ecosystem: coupling between daily cycles in solar flux, snowmelt, transpiration, groundwater, and streamflow at Sagehen Creek and Independence Creek, Sierra Nevada, USA. *Hydrol Earth Sys Sci* 24:5095–5123. <https://doi.org/10.5194/hess-24-5095-2020>
- Koshkin AL, Hatchett BJ, Nolin AW (2022) Wildfire impacts on western United States snowpacks. *Front Water* 4:971271. <https://doi.org/10.3389/frwa.2022.971271>
- Leonard RL, Kaplan LA, Elder JF, Coats RN, Goldman CR (1979) Nutrient transport in surface runoff from a subalpine watershed, Lake Tahoe Basin, California. *Ecolog Monogr* 49:281–310. <https://doi.org/10.2307/1942486>
- Lewis ASL, Mercado-Bettín D, Carey CC (2025) Ecological memory contributes to a spatial mismatch in water quality trends between the surface and bottom waters of 382 temperate lakes. *Ecol Lett* 28:e70243. <https://doi.org/10.1111/ele.70243>
- Loeb SL, Reuter JE, Goldman CR (1983) Littoral zone production of oligotrophic lakes. In: Wetzel RG (ed) *Periphyton of Freshwater Ecosystems*. Springer, Netherlands, Dordrecht, pp 161–167
- Loewen CJG (2023) Lakes as model systems for understanding global change. *Nat Clim Chang* 13:304–306. <https://doi.org/10.1038/s41558-023-01624-5>
- Loria K, Lowman H, Krause J, Katona L, Naranjo R, Scordo F, Harpold A, Chandra S, Blaszcak J (2025a) The influence of mountain streamflow on nearshore metabolism in a large, oligotrophic lake across drought and wet years. *Limnol Oceanogr* 70:2645–2659. <https://doi.org/10.1002/lno.70157>
- Loria K, Lowman H, Blaszcak J, Krause J (2025b) Nearshore high-frequency temporal water quality observations and process-based modeling of aquatic ecosystem metabolism in Lake Tahoe completed by members of the Blaszcak Lab at the University of Nevada Reno, 2021–2023 ver 2. *Environ Data Initiat*. <https://doi.org/10.6073/pasta/d53eb9b27cbd66c5a173c02cd1d67369>
- Loria, K., Lowman, H., Genzoli, L., Krause, J., Harpold, A., Chandra, S., Blaszcak, J., N.D. Mountain stream ecosystem metabolism and nitrogen cycling responses to hydroclimatic volatility. *Undergoing revision for Journal of Geophysical Research: Biogeosciences*.
- Lundquist JD, Cayan DR (2002) Seasonal and spatial patterns in diurnal cycles in streamflow in the Western United States. *J Hydrometeorol* 3:591–603. [https://doi.org/10.1175/1525-7541\(2002\)003%3c0591:SASPID%3e2.0.CO;2](https://doi.org/10.1175/1525-7541(2002)003%3c0591:SASPID%3e2.0.CO;2)

- MacIntyre S, Melack JM (1995) Vertical and horizontal transport in lakes: linking littoral, benthic, and pelagic habitats. *J N Am Benthol Soc* 14:599–615. <https://doi.org/10.2307/1467544>
- MacIntyre S, Romero JR, Kling GW (2002) Spatial-temporal variability in surface layer deepening and lateral advection in an embayment of Lake Victoria, East Africa. *Limnol Oceanogr* 47:656–671. <https://doi.org/10.4319/lo.2002.47.3.0656>
- Moser KA, Baron JS, Brahney J, Oleksy IA, Saros JE, Hundey EJ, Sadro S, Kopacek J, Sommaruga R, Kainz MJ, Strecker AL, Chandra S, Walters DM, Preston DL, Michelutti N, Lepori F, Spaulding SA, Christianson KR, Melack JM, Smol JP (2019) Mountain lakes: eyes on global environmental change. *Glob Planet Change* 178:77–95. <https://doi.org/10.1016/j.gloplacha.2019.04.001>
- Naranjo RC, Niswonger RG, Smith D, Rosenberry D, Chandra S (2019) Linkages between hydrology and seasonal variations of nutrients and periphyton in a large oligotrophic subalpine lake. *J Hydrol* 568:877–890. <https://doi.org/10.1016/j.jhydrol.2018.11.033>
- Natural Resources Conservation Service, 2024. Snow and Water Interactive Map. <https://www.nrcs.usda.gov/resources/data-and-reports/snow-and-water-interactive-map>
- Odum HR (1956) Primary production in flowing waters. *Limnol Oceanogr* 1:102–117. <https://doi.org/10.2307/2833008>
- Oleksy IA, Jones SE, Solomon CT (2022) Hydrologic setting dictates the sensitivity of ecosystem metabolism to climate variability in lakes. *Ecosystems* 25:1328–1345. <https://doi.org/10.1007/s10021-021-00718-5>
- Perga M, Bruel R, Rodriguez L, Guenand Y, Bouffard D (2018) Storm impacts on alpine lakes: antecedent weather conditions matter more than the event intensity. *Glob Change Biol* 24:5004–5016. <https://doi.org/10.1111/gcb.14384>
- R Core Team, 2024. R: A language and environment for statistical computing, v.4.4.1. R Foundation for Statistical Computing, Vienna, Austria. <https://www.R-project.org>
- Richardson DC, Carey CC, Bruesewitz DA, Weathers KC (2017) Intra- and inter-annual variability in metabolism in an oligotrophic lake. *Aquat Sci* 79:319–333. <https://doi.org/10.1007/s00027-016-0499-7>
- Roberts DC, Forrest AL, Sahoo GB, Hook SJ, Schladow SG (2018) Snowmelt timing as a determinant of lake inflow mixing. *Water Resour Res* 54:1237–1251. <https://doi.org/10.1002/2017WR021977>
- Sadro S, Melack JM (2012) The effect of an extreme rain event on the biogeochemistry and ecosystem metabolism of an oligotrophic high-elevation lake. *Arct Antarct Alp Res* 44:222–231. <https://doi.org/10.1657/1938-4246-44.2.222>
- Sadro S, Melack JM, MacIntyre S (2011) Spatial and temporal variability in the ecosystem metabolism of a high-elevation lake: integrating benthic and pelagic habitats. *Ecosystems* 14:1123–1140. <https://doi.org/10.1007/s10021-011-9471-5>
- Sakoe H, Chiba S (1978) Dynamic programming algorithm optimization for spoken word recognition. *IEEE Trans Acoust Speech Signal Process* 26:43–49. <https://doi.org/10.1109/TASSP.1978.1163055>
- Sardá-Espinosa A (2019) Time-series clustering in R using the dtwclust package. *R J* 11:22. <https://doi.org/10.32614/RJ-2019-023>
- Savoy P, Appling AP, Heffernan JB, Stets EG, Read JS, Harvey JW, Bernhardt ES (2019) Metabolic rhythms in flowing waters: an approach for classifying river productivity regimes. *Limnol Oceanogr* 64:1835–1851. <https://doi.org/10.1002/lno.11154>
- Scordo F, Sadro S, Culpepper J, Seitz C, Chandra S (2022) Wildfire smoke effects on lake-habitat specific metabolism: toward a conceptual understanding. *Geophys Res Lett* 49:e2021GL097057. <https://doi.org/10.1029/2021GL097057>
- Siirila-Woodburn ER, Rhoades AM, Hatchett BJ, Huning LS, Szinai J, Tague C, Nico PS, Feldman DR, Jones AD, Collins WD, Kaatz L (2021) A low-to-no snow future and its impacts on water resources in the Western United States. *Nat Rev Earth Environ* 2:800–819. <https://doi.org/10.1038/s43017-021-00219-y>
- Staehr PA, Bade D, Van De Bogert MC, Koch GR, Williamson C, Hanson P, Cole JJ, Kratz T (2010) Lake metabolism and the diel oxygen technique: state of the science. *Limnol Oceanogr Methods* 8:628–644. <https://doi.org/10.4319/lom.2010.8.0628>
- Swain DL, Prein AF, Abatzoglou JT, Albano CM, Brunner M, Diefenbaugh NS, Singh D, Skinner CB, Touma D (2025) Hydroclimate volatility on a warming Earth. *Nat Rev Earth Environ* 6:35–50. <https://doi.org/10.1038/s43017-024-00624-z>
- Ulseth AJ, Hall RO Jr., Boix Canadell M, Madiner HL, Niayifar A, Battin TJ (2019) Distinct air–water gas exchange regimes in low- and high-energy streams. *Nat Geosci* 12:259–263. <https://doi.org/10.1038/s41561-019-0324-8>
- Vadeboncoeur Y, Lowe R (2024) Benthic algae and cyanobacteria of the littoral zone. *Wetzel's limnology*. Elsevier, pp 817–857
- Vadeboncoeur Y, Moore MV, Stewart SD, Chandra S, Atkins KS, Baron JS, Bouma-Gregson K, Brothers S, Francoeur SN, Genzoli L, Higgins SN, Hilt S, Katona LR, Kelly D, Oleksy IA, Ozersky T, Power ME, Roberts D, Smits AP, Timoshkin O, Tromboni F, Zanden MJV, Volkova EA, Waters S, Wood SA, Yamamuro M (2021) Blue waters, green bottoms: benthic filamentous algal blooms are an emerging threat to clear lakes worldwide. *Bioscience* 71:1011–1027. <https://doi.org/10.1093/biosci/biab049>
- Wang W, Zhang Y (2007) On fuzzy cluster validity indices. *Fuzzy Sets Syst* 158:2095–2117. <https://doi.org/10.1016/j.fss.2007.03.004>
- Ward NK, Brentrup JA, Richardson DC, Weathers KC, Hanson PC, Hewitt RJ, Carey CC (2022) Dynamics of the stream–lake transitional zone affect littoral lake metabolism. *Aquat Sci* 84:31. <https://doi.org/10.1007/s00027-022-00854-7>
- Williamson CE, Saros JE, Vincent WF, Smol JP (2009) Lakes and reservoirs as sentinels, integrators, and regulators of climate change. *Limnol Oceanogr* 54:2273–2282. https://doi.org/10.4319/lo.2009.54.6_part_2.2273
- Woolway RI, Kraemer BM, Lenters JD, Merchant CJ, O'Reilly CM, Sharma S (2020) Global lake responses to climate change. *Nat Rev Earth Environ* 1:388–403. <https://doi.org/10.1038/s43017-020-0067-5>
- Xia Y, Mitchell K, Ek M, Sheffield J, Cosgrove B, Wood E, Luo L, Alonge C, Wei H, Meng J, Livneh B, Lettenmaier D, Koren V, Duan Q, Mo K, Fan Y, Mocko D (2012) Continental-scale water and energy flux analysis and validation for the North American Land Data Assimilation System project phase 2 (NLDAS-2): 1. Intercomparison and application of model products water and energy flux analysis. *J Geophys Res: Atmosph*. <https://doi.org/10.1029/2011JD016048>

Publisher's Note Springer Nature remains neutral with regard to jurisdictional claims in published maps and institutional affiliations.

Springer Nature or its licensor (e.g. a society or other partner) holds exclusive rights to this article under a publishing agreement with the author(s) or other rightsholder(s); author self-archiving of the accepted manuscript version of this article is solely governed by the terms of such publishing agreement and applicable law.